Development 136, 1621-1631 (2009) doi:10.1242/dev.020735

Mutations in zebrafish leucine-rich repeat-containing six-like affect cilia motility and result in pronephric cysts, but have variable effects on left-right patterning

Fabrizio C. Serluca[1,*,†,‡], Bo Xu[2,*], Noriko Okabe[2], Kari Baker[2], Shin-Yi Lin[2], Jessica Sullivan-Brown[2], David J. Konieczkowski[2], Kimberly M. Jaffe[2], Joshua M. Bradner[2], Mark C. Fishman[1,†] and Rebecca D. Burdine[2,‡]

Cilia defects have been implicated in a variety of human diseases and genetic disorders, but how cilia motility contributes to these phenotypes is still unknown. To further our understanding of how cilia function in development, we have cloned and characterized two alleles of *seahorse*, a zebrafish mutation that results in pronephric cysts. *seahorse* encodes Lrrc6l, a leucine-rich repeat-containing protein that is highly conserved in organisms that have motile cilia. *seahorse* is expressed in zebrafish tissues known to contain motile cilia. Although mutants do not affect cilia structure and retain the ability to interact with Disheveled, both alleles of *seahorse* strongly affect cilia motility in the zebrafish pronephros and neural tube. Intriguingly, although *seahorse* mutations variably affect fluid flow in Kupffer's vesicle, they can have very weak effects on left-right patterning. Combined with recently published results, our alleles suggest that the function of *seahorse* in cilia motility is separable from its function in other cilia-related phenotypes.

KEY WORDS: Zebrafish, *seahorse*, Lrrc6l, Cilia motility, Asymmetry, Pronephros, Cysts, Kupffer's vesicle

INTRODUCTION

Ciliary motility disorders are known to cause a spectrum of diseases in humans, including chronic respiratory disorders, increased rates of situs inversus and male infertility (reviewed by Fliegauf et al., 2007). Defects in ciliary structure and function have also been implicated in mammalian cystic kidney disease (Yoder, 2007). In the mammalian kidney, cells produce a single primary cilium that extends into the renal lumen. This cilium is thought to function in cell signaling events and/or to sense and respond to luminal flow (Praetorius and Spring, 2005).

Similarly, studies in zebrafish have shown that cilia motility and structure are essential for proper kidney development, and that early defects in cilia correlate with pronephric cyst formation (Kramer-Zucker et al., 2005; Omori and Malicki, 2006; Sullivan-Brown et al., 2007; Zhao and Malicki, 2007). In contrast to the immotile cilia observed in the mammalian kidney, the cilia in the zebrafish pronephros are motile and thought to regulate fluid exit from the body (Kramer-Zucker et al., 2005). When fluid flow is disrupted in zebrafish, cyst formation can occur. However, recent research suggests that cilia function may have even earlier roles in regulating kidney morphogenesis (Sullivan-Brown et al., 2007).

Cilia motility has also been implicated in the specification of the left-right axis in both zebrafish and mammals (reviewed by Bisgrove and Yost, 2006). In vertebrates, a transient ciliated structure known as the node in mammals and Kupffer's vesicle (KV) in zebrafish is essential for proper left-right axis development. Severe defects in cilia motility within the node/KV result in incorrect expression of the normally left-sided gene *nodal*, which subsequently results in abnormal placement of organs about the left-right axis. Without cilia motility, directional flow of fluid inside the node/KV fails to occur (Essner et al., 2005; Kramer-Zucker et al., 2005; Okada et al., 1999), but the specific mechanism of how directional fluid flow within the node/KV restricts *nodal* expression to the left side of the organism remains unclear.

Because cilia defects result in a large and diverse group of disorders, it is important to understand the molecular and cellular basis of how cilia motility, structure and function influence physiology and development. We have taken the approach of cloning and characterizing genes that function in pathways influenced by cilia. These genes will give us a starting point for determining the downstream signaling pathways regulated by cilia and will provide insights into the structure and function of cilia components. Here, we report the cloning and characterization of two alleles of zebrafish *seahorse* (*sea*), *sea*^{tg238a} and *sea*^{fa20r}, that have been isolated from two independent screens. *sea* encodes a leucine-rich repeat-containing protein, Lrrc6l. We show that the above mutations in *lrrc6l* do not affect cilia structure, apical position of the basal body or the ability to interact with Disheveled, but result in severe cilia motility defects in the pronephros and neural tube that range from slow and disorganized cilia motility to immotile cilia. Although these two *sea* alleles result in a fully penetrant pronephric cyst phenotype, they surprisingly show a low incidence of left-right patterning defects. *sea* mutants have variable effects on fluid flow in KV, ranging from loss of flow, to flow that is indistinguishable from wild type. Thus, here we provide the first experimental evidence that *lrrc6l* is required for cilia motility in vivo. Although these mutations affect cilia motility, they have different effects on downstream cilia-related phenotypes, thereby showing that the function of Sea in cilia motility and cilia-related phenotypes is genetically separable.

[1]Cardiovascular Research Center, Massachusetts General Hospital, 149 13th Street, Charlestown, MA 02129, USA. [2]Princeton University, Department of Molecular Biology, Princeton, NJ 08544, USA.

*These authors contributed equally to this work
[†]Present address: Novartis Institutes for Biomedical Research, Cambridge, MA 02139, USA
[‡]Authors for correspondence (e-mail: fabrizio.serluca@novartis.com; rburdine@princeton.edu)

Accepted 16 March 2009

MATERIALS AND METHODS

Positional cloning of *sea*

Mapping was performed as described previously (Liao and Zon, 1999). Initial linkage to chromosome 2 was found using marker Z1406 and the region narrowed using additional markers. The closest marker, Z8448, was used to initiate a BAC walk towards the mutation as described (Liao and Zon, 1999). To determine the molecular lesions in each allele, mutant cDNAs or genomic DNAs were amplified and subjected to sequencing (details of primer sequences are available upon request).

In silico analysis

GCG SeqWeb version 1.1 was used to identify the presence of leucine-rich repeats (MEME) and coiled-coil domain (CoilScan). Protein alignments were performed by NCBI BLAST (Blosum 62 substitution matrix). PSORT II (http://psort.ims.u-tokyo.ac.jp) was used to identify nuclear localization signals and CBS NetNES algorithm (http://www.cbs.dtu.dk/services/NetNES) was used to identify nuclear export signals.

sea cDNA cloning

The published cDNA for *sea* (NCBI AY618925) contains a 101 bp 5′ UTR, a 1323 bp coding sequence and a 334 bp 3′ UTR. A search of The Institute for Genomic Research (TIGR) expressed sequence tag database revealed a possible 168 bp extension (cluster fj66c12.x1 AW077770) beyond the published 3′ UTR terminus. Primers based on the extended sequence amplified the *sea* cDNA using Expand Hi-fidelity enzyme (Roche, Indianapolis, IN, USA) and a zebrafish 24 hpf cDNA library constructed using the Marathon cDNA Amplification Kit (Clontech, Mountain View, CA USA). The 1.9 kb product was amplified, confirming the authenticity of the 3′UTR extension, and subcloned into pBluescript SKII(+) (Stratagene, La Jolla, CA USA) creating plasmid BL289.

In vitro transcription and in situ hybridization

mRNA transcripts were synthesized using mMessage mMachine kits (Ambion, Austin TX, USA) and quantified by UV spectrophotometry. Plasmid BL289 was linearized with *Not*I and transcribed using T3 RNA polymerase, and 500 pg of mRNA per embryo was injected at the one-cell stage. Plasmid BL355, containing a partial *sea* cDNA, was linearized with *Not*I and transcribed with T7 RNA polymerase to generate antisense in situ hybridization probe. In situ hybridization was performed as previously described (Thisse et al., 1993). Probes used include: *southpaw* (Long et al., 2003), *cardiac myosin light chain (cmlc2/myl7)* (Yelon et al., 1999), *forkhead 2* (*fkd2/foxa3*) (Odenthal and Nusslein-Volhard, 1998), *preproinsulin* (Milewski et al., 1998), *lefty1* and *lefty2* (Bisgrove et al., 1999), *lov* (Gamse et al., 2003), *wt1* (Bollig et al., 2006; Serluca and Fishman, 2001), *pax2.1* (Krauss et al., 1991), and *α-tropomyosin* (Ohara et al., 1989).

Morpholinos and RT-PCR

Four different morpholino antisense oligonucleotides (MO1-MO4) directed against *sea* were purchased from GENE Tools (Philomath, OR USA; sequences available upon request). Only MO1 (seae5i5) 5′-TTAGACACTCACTGGTTTATTTCAG-3′ gave specific phenotypes upon injection, and thus was used in this report. MO1 (2 nl of 1 mM) was injected into one-cell stage embryos for phenocopy experiments. For low-level MO injections, 400 pl of 1 mM MO1 was injected. To determine the extent of splice blocking, RT-PCR was performed and the resulting products were sequenced. cDNA libraries used in RT-PCR to determine stage of *sea* expression or extent of MO splice-blocking were created from total RNA with the SuperScript First-Strand Synthesis System (Invitrogen, Carlsbad, CA, USA).

Genotyping

PCR was performed on DNA extracted from embryos or fin clips using primers for sea^{tg238a} (5′-TTTGCTTGAAAAGTGTGATGTGA-3′ and 5′-AAGGTTGTGCTTCAGCG-3′) or for sea^{fa20r} (5′-CAGAGAACTTG-TACCTGTGTTTTGGATGAA-3′ and 5′-TCTCCCAGAATTCCCTCTC-CTCG-3′). The *fa20r* mutation creates an *Alu*I restriction site, which cleaves the 114 bp PCR product into 81 bp and 33 bp fragments (Fig. 1C,C′,D). The *tg238a* mutation abolishes the *Fsp*BI site preventing cleavage of a 176 bp fragment into 114 and 62 bp fragments (Fig. 1C′,C″,D′).

Histology and immunohistochemistry

Immunostaining for the Na^+/K^+ ATPase and acetylated tubulin were performed as described (Sullivan-Brown et al., 2007). Nuclei were stained with DRAQ5 (Axxora, San Diego, CA USA). Histological analysis and sectioning of immunostained embryos were performed as described previously (Sullivan-Brown et al., 2007).

Co-immunoprecipitation

HA epitope-tagged *sea* wild-type and mutant cDNAs were cloned into pcDNA3.1 (Invitrogen, Carlsbad, CA USA) using standard methods. Flag-tagged Disheveled has been described previously (Habas et al., 2001). For immunoprecipitation assays, wild-type or mutant Seahorse proteins were expressed in the presence or absence of Disheveled in Cos-7 cells using Lipofectamine2000 transfection (Invitrogen, Carlsbad, CA USA). Cells were lysed in a modified RIPA buffer [50 mM Tris (pH 7.4), 150 mM NaCl, 0.5% NP-40, 0.25% deoxycholic acid, 1 mM EDTA, 1 mM NaF] supplemented with 0.4 mM PMSF and Complete Mini Protease inhibitor cocktail (Roche, Indianapolis, IN USA). The immunoprecipitation antibody (α-Flag AP M2, Sigma-Aldrich, St Louis MO, USA) was added to the lysates at a dilution of 1:500 and incubated at 4°C for 2 hours. Protein A-Sepharose beads (Sigma-Aldrich, St Louis MO, USA) were added to the lysates and gently rocked for an additional two hours at 4°C. The bead complexes were washed with modified RIPA buffer, mixed with SDS-sample buffer, boiled and spun. All supernatants were resolved on Nu-PAGE 10% Bis-Tris Gels (Invitrogen, Carlsbad, CA USA) and proteins detected using primary antibodies, coupled with horseradish peroxidase, against the epitope tags (Anti-HA-HRP clone 3F10, Roche, Indianapolis, IN USA; Anti-Flag-HRP clone M2, Sigma-Aldrich, St Louis MO, USA). Proteins were detected using LumiLight Plus (Roche, Indianapolis, IN, USA).

Microscopy

Embryos processed for immunofluorescence were visualized on a Zeiss LSM 510. For analysis of KV cilia, embryos were mounted in 50% glycerol in PBS, and imaged. Cilia lengths were obtained using ImageJ to analyze re-plotted iz-stacks. Embryos processed for RNA in situ hybridization were photographed as described (Schottenfeld et al., 2007). Cilia motility imaging in the pronephros was performed as described (Sullivan-Brown et al., 2007). Embryos (48 hpf) were processed for transmission electron microscopy as described (Majumdar and Drummond, 2000) and imaged on the Zeiss 921AB.

Analysis of KV fluid flow

Beads were injected in KV and movement analyzed at the six-somite stage as described (Essner et al., 2005; Okabe and Burdine, 2008). After imaging, embryos were raised to 48 hpf to distinguish mutants from siblings using the CTD phenotype and heart looping was scored. Defects in fluid flow were annotated using a blind test involving nine people who analyzed unlabeled movies from *sea* siblings or mutants compared with wild-type embryos. Flow is annotated as described previously (Essner et al., 2005).

RESULTS

Mutations in *seahorse* consistently result in body curvature defects and pronephric cysts

tg238a was isolated in a large-scale screen conducted in Tübingen as a curly tail down (CTD) mutant with pronephric cysts (Brand et al., 1996). *fa20r* was isolated in an independent F3 screen for pronephric cyst mutations [as previously described in Chen et al. (Chen et al., 2001)]. Complementation crosses between *fa20r* and *tg238a* heterozygous parents resulted in 25% CTD F1 embryos with pronephric cysts, confirming that the mutations were allelic (data not shown). The gene mutated in *fa20r* and *tg238a* was independently cloned in a retroviral insertional mutagenesis screen for genes causing pronephric cysts (Sun et al., 2004) and named

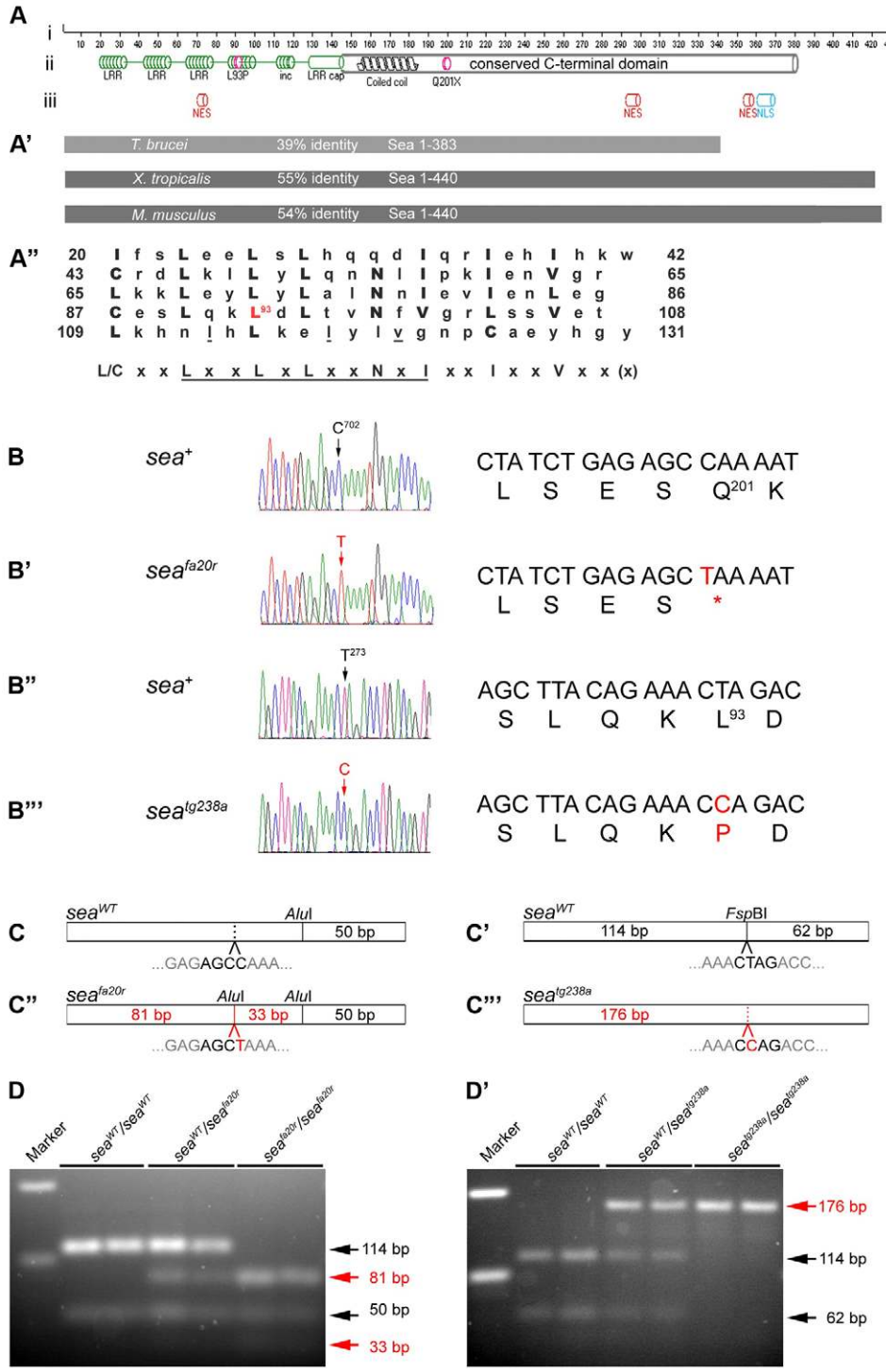

Fig. 1. *seahorse* encodes Lrrc6l. (**A-A″**) *sea* encodes a 440 amino acid protein (Ai); the N terminus contains four LRR motifs terminated by an LRR cap motif (green; Aii). The fourth LRR motif is disrupted by the *sea*^{tg238a} L93P missense mutation (pink). *sea*^{fa20r} Q201X nonsense mutation truncates the protein shortly after the coiled-coil (pink). The protein is predicted to contain three weak nuclear export signals (NES) and one strong nuclear localization signal (Aiii). (A′) Lrrc6l is conserved among species. An ortholog from *T. brucei* is 39% identical to amino acids 1-363 of Sea. Orthologs from *Xenopus* and mouse are 55% identical and 54% to amino acids 1-440 of Lrrc6l, respectively, and extend roughly 30 amino acids beyond the Lrrc6l C terminus. (A″) Alignment of the four Lrrc6l LRR motifs; the consensus Lrrc6l LRR sequence is [L/C]xxLxxLxxNxIxxIxxVxx(x) and is most similar to repeats in the SDS22-like subfamily (Kobe and Kajava, 2001). The core LRR consensus sequence shared among all LRR proteins, LxxLxLxxN/CxL (x can be any amino acid and L positions can be V, I or F), is underlined (Kobe and Kajava, 2001). (**B-B‴**) *sea*^{fa20r} is a 702C→T transition in exon 5 encoding a Q201X truncation (B,B′). *sea*^{tg238a} is a 273T→C transition in exon 3 encoding an L93P missense (B″,B‴). (**C-C‴**) Genotyping (C,C″) *sea*^{fa20r} (red) creates an *Alu*I restriction site (black nucleotides), cleaving the 114 base pair (bp) PCR product into 81 and 33 bp fragments. (C′,C‴) *sea*^{tg238a} (red) abolishes an *Fsp*BI restriction site (black nucleotides), preventing cleavage of the 176 bp fragment into 114 and 62 bp fragments. (**D**,**D′**) Genotyping results. The left-most lanes contain DNA size markers with upper band at 200 bp and lower band at 100 bp.

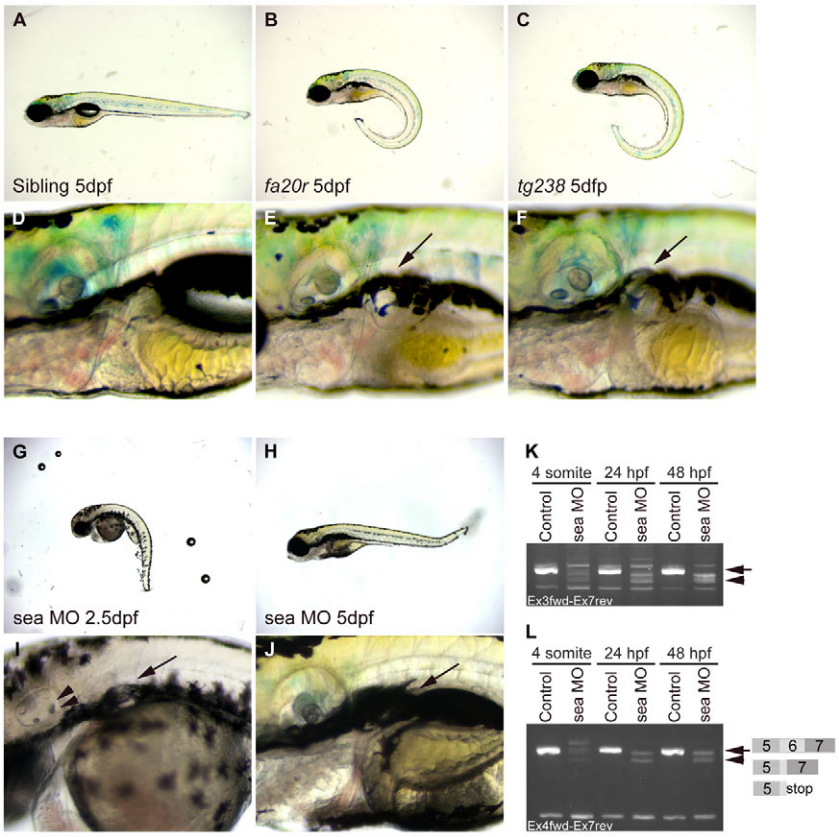

Fig. 2. *seahorse* mutants and sea MO-injected embryos displayed curly tail down and pronephric cyst phenotypes. (**A-F**) CTD and pronephric cyst phenotypes in *sea* mutants. (A) Siblings, (B) *sea*^{fa20r} and (C) *sea*^{tg238a}; mutant embryos have CTD phenotypes at 5 dpf. (D) Siblings, (E) *sea*^{fa20r} and (F) *sea*^{tg238a} embryos at higher magnification to show pronephric cysts at 5 dpf (arrows). (**G-J**) CTD and pronephric cyst phenotypes in sea MO-injected embryos. MO-injected embryos can recover from the CTD (H) and cyst phenotypes (J) by 5 dpf. Defects in otic vesicle and otolith formation (arrowheads) were observed in some sea MO-injected embryos (I). (**K**,**L**) RT-PCR from uninjected and sea MO-injected cDNA libraries at four somites, 24 hpf and 48 hpf. (K) Primers between exon 3 and exon 7 amplified a wild-type *sea* band at 635 base pairs (bp; arrow) and incorrectly spliced message in *sea* MO-injected embryos (arrowhead). (L) Primers between exon 4 and exon 7 amplified a wild-type *sea* band at 517 bp (arrow; exon 5-7) and incorrectly spliced message in *sea* MO-injected embryos (arrowhead). Incorrect splicing generated two main splice forms creating either a deletion and/or stop codon in exon 6 (indicated by the diagram in L).

seahorse (*sea*, NCBI AY618925). Thus, we will refer to our alleles as *sea*^{fa20r} and *sea*^{tg238a}. The CTD phenotype in *sea*^{fa20r} and *sea*^{tg238a} embryos is first detectable at 27 hours post fertilization (hpf) and persists through later stages (data not shown and Fig. 2A-C). Both alleles develop pronephric cysts that are morphologically visible in all mutant embryos by 3.5 dpf (Table 1; Fig. 2D-F; and data not shown).

seahorse encodes Leucine-rich repeat-containing 6 like (Lrrc6l)

We cloned the gene affected in *sea* using standard methods. *lrrc6l* was located in the smallest genetic interval and was a likely candidate based on mapping data and the presence of this gene in the cilia proteome (Avidor-Reiss et al., 2004). Lrrc6l is a leucine-rich repeat-containing protein of 440 amino acids with a predicted

Table 1. Phenotypes of *sea* mutants, morphants and mRNA-rescued embryos

Genotype	Age (dpf)	*n*	Tail phenotypes (%)			Pronephric phenotypes (%)	
			Straight	CTD	Abnormal	None	Cysts
sea^{fa20r} siblings (+/+, +/–)	2.5	96	100	–	–	100	–
sea^{fa20r} –/–	2.5	36	–	100	–	31	69
sea^{fa20r} –/–	3.5	36	–	100	–	–	100
Wild type + e5i5 sea MO	1.5	140	14	84	2	n/a	n/a
Wild type + e5i5 sea MO	2.5	127	45	55	–	29	71
Wild type + e5i5 sea MO	3.5	127	78	22	–	48	52
sea^{fa20r} clutch	1.5	78	73	27	–	n/a	n/a
sea^{fa20r} clutch + mRNA	1.5	118	100	–	–	n/a	n/a
sea^{fa20r} clutch	2.5	78	73	27	–	73	27
sea^{fa20r} clutch + mRNA	2.5	118	98	–	2	92	8
sea^{tg238a} clutch	1.5	292	74	26	–	n/a	n/a
sea^{tg238a} clutch + mRNA	1.5	52	94	6	–	n/a	n/a
sea^{tg238a} clutch	2.5	25	76	24	–	80	20
sea^{tg238a} clutch + mRNA	2.5	45	96	4	–	96	4

dpf, days post fertilization; CTD, curly tail down.
Abnormal refers to a small percentage of embryos that showed various developmental defects upon injection of the e5i5 MO. These defects were not observed in uninjected controls. The same MO embryos analyzed at 2.5 dpf were analyzed at 3.5 dpf. The 2% abnormal embryos seen in the fa20r clutch injected with mRNA refer to a few embryos that had a curly tail up phenotype. In clutches of embryos, we expect 25% to be mutants.

molecular weight of 50.5 kDa. MEME repeat searching identified four leucine-rich repeat (LRR) protein-protein interaction motifs present near the N terminus (Fig. 1Aii, green). The 22-32 amino acid consensus LRR in Lrrc6l includes the canonical repeat shared among all LRR proteins (Fig. 1A″, underline). The full LRR repeat region in Lrrc6l most closely resembles that of the SDS22-like subfamily of LRR proteins (Kobe and Kajava, 2001; Ohkura and Yanagida, 1991). Amino acids 131-146 encode the LRR cap (Ceulemans et al., 1999), a motif that terminates LRR domains in many LRR-containing proteins. Immediately after the LRR cap motif, a coiled-coil domain was predicted between 148 and 186 amino acids (Fig. 1Aii). The protein contains a possible nuclear localization signal (NLS) at 363-369 amino acids and three weak nuclear export signals (NESs) at 73-75, 295-299 and 356-358 amino acids (Fig. 1Aiii). Lrrc6l is significantly conserved among species (Fig. 1A′). Amino acids 1-383 of Lrrc6l are homologous (39% identity, 58% similarity) to an LRR-containing protein from *T. brucei* (AAF73195) (Morgan et al., 2005). Full-length Lrrc6l had 55% identity to *X. tropicalis* LRRC6 (CAJ83438.1) and 54% identity to mouse LRRC6 (AAH46277.1) (Xue and Goldberg, 2000). Both *Xenopus* and mouse orthologs extended roughly 30 amino acids beyond the C terminus of zebrafish Lrrc6l (Fig. 1A′).

Both *sea* alleles were sequenced to determine the molecular lesions in Lrrc6l. The *fa20r* mutation encodes a Q201X truncation that occurs after the predicted coiled-coil domain (Fig. 1A,B,B′). The *tg238a* encodes a L93P missense mutation within the fourth LRR (Fig. 1A,B″,B‴). Injection of sea^{tg238a} or sea^{fa20r} clutches with *lrrc6l* mRNA was able to rescue both the CTD and pronephric cyst phenotypes at 1.5 dpf and 2.5 dpf, respectively (Table 1). Finally, a morpholino directed against the exon/intron boundary of exon 5 (e5i5) phenocopied *sea* mutants with variable degrees of CTD and visible pronephric cysts (Table 1; Fig. 2G-J). These effects were most obvious at 1.5 dpf and 2.5 dpf, respectively. By 3.5dpf, 52% of the embryos retained cysts whereas the majority no longer displayed a CTD phenotype and even fewer resembled *sea* mutants at 5 dpf (Fig. 2H,J; and data not shown). This suggests that the injected MO is not able to maintain knockdown to later stages and that the MO-injected embryos can recover from both the tail curl and pronephric cyst formation. We confirmed the effects of the morpholinos on splicing by RT-PCR on MO-injected embryos at four somites, 24 hpf and 48 hpf (Fig. 2K,L).

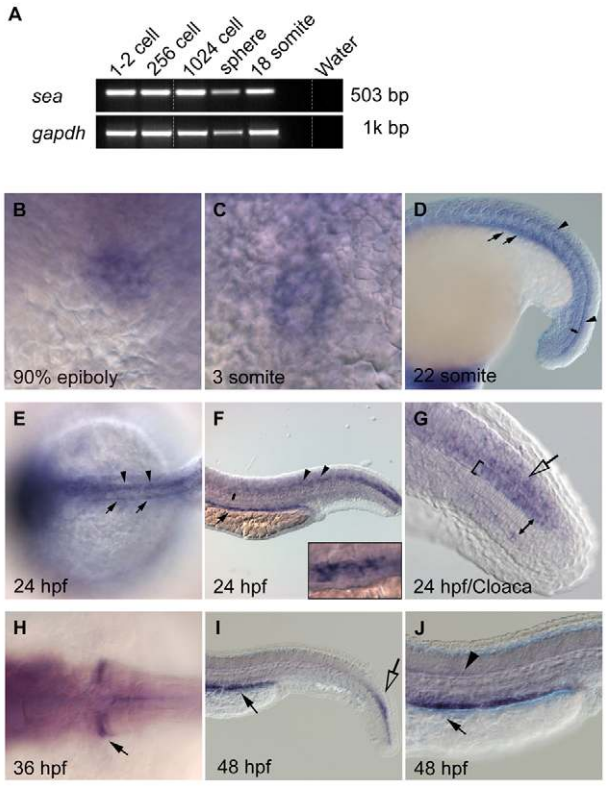

Fig. 3. *seahorse* mRNA is expressed in tissues that possess motile cilia. (**A**) RT-PCR of *sea* mRNA (503 bp) in cDNA libraries at the one- to two-cell, 256-cell, 1024-cell, sphere and 18-somite stages. *sea* mRNA was maternally expressed as zygotic transcription initiates after the 1024-cell stage. (**B-J**) Expression of *sea* was detected by RNA in situ hybridization in dorsal forerunner cells at 90% epiboly (B), in KV at 3 somites (C), and in the floor plate at 22 somites (D, arrowheads), 24 hpf (E,F arrowheads; G, bracket) and 48 hpf (J, arrowhead). Expression was detected in the pronephric tubules at 22 somites (D, arrows), 24 hpf (E,F, arrows), 36 hpf (H, arrow) and at 48 hpf (I,J, arrow). Open arrows in G and I indicate *sea* expression in the chordoneural hinge. Double-headed arrows in D,F and G span the width of the notochord, *sea* mRNA is not detected. Inset in F is a higher magnification image of the patchy pronephric expression that resembles expression of genes in multiciliated cells (Liu et al., 2007; Ma and Jiang, 2007).

seahorse expression pattern suggests a role for Lrrc6l in cilia motility

To determine when and where *sea* may function during development, we analyzed *sea* mRNA expression in wild-type embryos. By RT-PCR, *sea* is expressed both maternally and zygotically (Fig. 3A). Consistent with our RT-PCR experiments, a low level of expression was detected by RNA in situ hybridization at 256-cell, sphere and 30-50% epiboly stages, indicating that *sea* is maternally provided (data not shown). Specific expression was observed in the dorsal forerunner cells (Fig. 3B) and in KV (Fig. 3C). During mid to late somitogenesis, *sea* mRNA was also detected in the floor plate (Fig. 3D). After 24 hpf, *sea* expression in the floor plate was weaker in the anterior regions but stronger at the posterior end of the tail (Fig. 3F,G,I), expanding into the chordoneural hinge (Fig. 3G). *sea* was expressed in the pronephric tubules from mid-somitogenesis through 48 hpf (Fig. 3D-F,H-J).

All of these locations contain motile cilia (Kramer-Zucker et al., 2005) (this report). As further support that *sea* may be involved in cilia motility, *sea* is expressed in a patchy pattern within the pronephros (Fig. 3F, inset), a pattern similar to other genes expressed in multiciliated cells in this region (Liu et al., 2007; Ma and Jiang, 2007). Furthermore, at 36 hpf, *sea* expression localizes to the anteriormost tubules adjacent to the glomerular region (Fig. 3H), which may correspond to the ciliary neck segment found in mammals and other teleosts (Wingert et al., 2007).

seahorse mutations result in pronephric cyst formation

sea mutants develop pronephric cysts, observable by light microscopy in living embryos between 2.5 dpf and 3 dpf (Table 1; Fig. 2). Early patterning of the pronephros was unaffected in *sea* based on correct expression of *wt1* at eight somites and *pax2.1* at eight somites and 48 hpf (Fig. 4A-F) (Serluca and Fishman, 2001). However, at 3dpf variable effects on *wt1* expression were observed in *sea*. In sibling embryos, *wt1* expression was condensed within the fused glomerular region (Fig. 4I). In mutant embryos, the *wt1* expression was more diffuse ranging from slight (Fig. 4J) to extreme

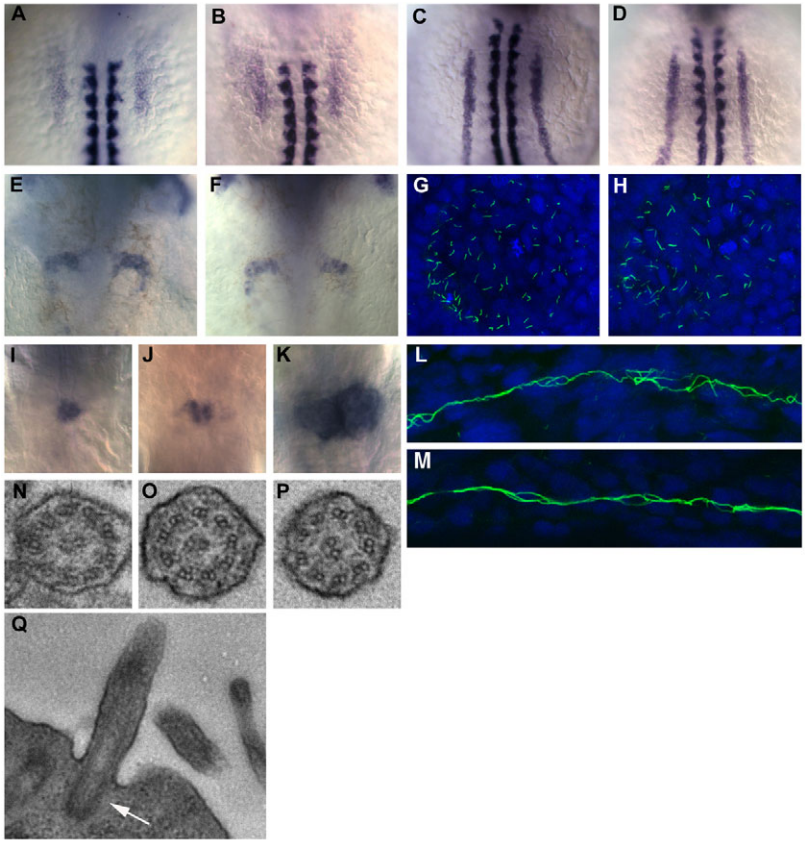

Fig. 4. Mutations in *lrr6l* do not affect general pronephric patterning or cilia structure. (**A-D**) Expression of pronephric specification genes at eight somites is not affected in *sea* mutants (B,D) compared with wild type (A,C). (A,B) *wt1* is correctly expressed in the intermediate mesoderm from the first somite to the beginning of the fourth somite. (C,D) *pax2.1* is correctly expressed in the intermediate mesoderm posterior to the third somite. In A-D, RNA in situ hybridization for *α-tropomyosin* was used to visualize the somites. (**E**,**F**) Expression of *pax2.1* in the neck segments at 48 hpf is unaffected in *sea* mutants (F) compared with siblings (E). (**G**,**H**) Acetylated tubulin immunofluorescence of KV at six somites in *sea* mutant (H) and sibling (G) shows that cilia are not affected in *sea* mutants. (**I-K**) In wild-type embryos at 72 hpf (I), *wt1* is expressed in the fused glomerulus in the midline. In *sea* mutants, defects in *wt1* expression were seen, including separation of the glomeruli (J) and drastic expansions of the *wt1* domain (K). These effects are probably caused by the expansion of the glomerular region. (**L**,**M**) Acetylated tubulin staining in sibling (L) and *sea* mutants (M) at 27 hpf indicate that cilia formation in the pronephros is unaffected by mutations in *sea*. All above images are from sea^{fa20r} mutants, but similar results were obtained for sea^{tg238a}. (**N-Q**) TEM analysis of pronephric cilia show no alterations in axoneme structure in sea^{fa20r} mutants (O,P) compared with siblings (N). Basal body localization at the apical membrane is also unaffected in sea mutants (Q; arrow indicates basal body). Anterior is towards the top in A-K. L and M are lateral views of the pronephric tubules; anterior is towards the left.

expansion (Fig. 4K). The expansion of *wt1* expression is probably an indirect/secondary consequence of the dilations that form in this region (see below).

We performed a histological time course to determine when and where cyst formation begins in *sea* mutants. At 2 dpf, the glomeruli in *sea* mutants often appeared unaffected, similar to those in siblings (Fig. 5A,B). By contrast, the medial tubules (posterior to the glomerulus), were always dilated in the *sea* mutants at 2 dpf (Fig. 5D,E). By 2.5 dpf, dilations can be detected in the glomeruli and medial tubules of all *sea* mutants (Fig. 5G,H,J,K). A number of different phenotypes have been associated with cyst formation in zebrafish, including disrupted apical-basal localization of the Na^+/K^+-ATPase (Drummond, 2003). Consistent with other cystic mutants, *sea* mutants did not show a normal pattern of basolateral Na^+/K^+-ATPase localization at 3 dpf based on immunofluorescence (Fig. 5M-O). Overall, these results are consistent with those we obtained for other mutants with cilia motility defects (Sullivan-Brown et al., 2007).

seahorse mutations strongly affect cilia motility in the pronephros and neural tube

We have shown that defects in cilia motility precede tubule dilations (Sullivan-Brown et al., 2007). To analyze cilia motility in *sea*, video recordings of cilia movement were performed as previously described (Sullivan-Brown et al., 2007). In sibling embryos, cilia are motile in the pronephric tubules (30 hpf) (see Movies 1 and 2 in the supplementary material), the cloaca (2 dpf) (Movie 3 in the supplementary material) and in the neural tube (2 dpf) (Movie 4 in the supplementary material). At later time points, cilia in the medial tubules bundle and display a coordinated movement (3 dpf) (Movie 5 in the supplementary material) (Sullivan-Brown et al., 2007). By contrast, the motility of *sea* mutant cilia at these same time points and locations was affected in all embryos observed, and ranged from slow and disorganized to completely immotile (see Movies 6-10 in the supplementary material). This result suggests that *sea* plays a crucial role in regulating cilia motility in these tissues. To determine whether *sea* mutations also affect cilia formation, we performed immunofluorescence for acetylated tubulin. No differences in cilia length or number were observed in the pronephros of *sea* mutants (Fig. 4L,M). To confirm that *sea* mutations do not affect cilia structure, we performed TEM analysis of cilia within the pronephros and found no differences in axoneme structure between mutants and siblings (Fig. 4N-P).

seahorse mutations have weak effects on left-right patterning

Other zebrafish mutants with CTD and pronephric cyst phenotypes also have defects in left-right patterning. This combination of phenotypes is not surprising as these mutations often affect cilia, and cilia have been implicated both in cyst development and left-right patterning (reviewed by Bisgrove and Yost, 2006). As *sea* is expressed in KV and affects cilia motility, we analyzed left-right patterning in both alleles.

We analyzed visceral organ placement (Schottenfeld et al., 2007) and asymmetric *lov* expression in the brain (Gamse et al., 2003) (see Fig. S1 in the supplementary material). Surprisingly, we found that visceral organ asymmetry was only affected in 9-11% of *sea* mutant embryos (Table 2; see Table S1 in the supplementary material). *sea* mutants showed a similarly low level of defects in brain asymmetry (17-29%) (Table 3). These numbers are much lower than what we observe in other mutants

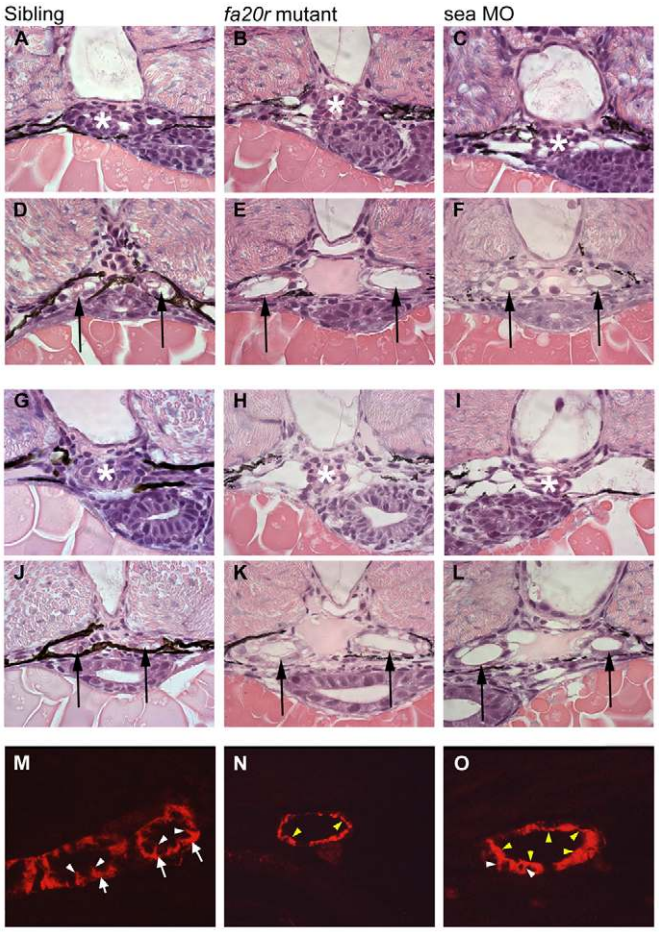

Fig. 5. Pronephric cyst phenotypes in *seahorse* mutants and sea MO-injected embryos. (**A-F**) At 2 dpf, the glomerular region (asterisks) appears normal in siblings (A) and *sea*^{fa20r} mutants (B), and slightly dilated in *sea* MO-injected embryos (C). In the same embryos, the medial tubules (arrows) were significantly dilated both in *sea*^{fa20r} mutants (E) and sea MO-injected embryos (F), compared with siblings (D). (**G-L**) At 2.5 dpf, the glomeruli (asterisks) in both the *sea*^{fa20r} mutants (H) and sea MO-injected embryos (I) were dilated compared with siblings (G). These same embryos have dilations in the medial tubules (arrows) in *sea*^{fa20r} mutants (K) and sea MO-injected embryos (L) compared with siblings (J). (**M-O**) At 3 dpf, siblings (M) display basolateral localization of Na^+/K^+-ATPase (red) in the pronephric epithelium (arrows; white arrowheads indicate lateral staining), whereas the *sea* mutants (N,O) display altered localization of Na^+/K^+-ATPase diffusely at apical (yellow arrowheads) and lateral membranes (white arrowheads).

we have analyzed, such as *curly up* (*pkd2*), where 65% of mutants display visceral organ defects and 59% display defects in brain asymmetry (Schottenfeld et al., 2007).

Correct left-right placement of organs requires proper left-sided expression of Nodal pathway components earlier in development. To determine whether the low level of visceral and brain asymmetry defects in *sea* mutants was preceded by a low level of abnormal Nodal gene expression, we assayed the expression of *southpaw, lefty1* and *lefty2* at 20 somites (see Fig. S1 in the supplementary material). Indeed, *sea* mutants do have a low level of asymmetric gene expression defects (Table 2). Thus, we conclude that *sea* mutations have a slight defect in left-right patterning over background.

seahorse mutations have variable effects on KV fluid flow

Even though *sea* strongly affects cilia motility and kidney development, *sea* may either play a less crucial role in left-right patterning than other cilia mutants, or have less of an effect on cilia formation and motility in KV. To analyze the effect of *sea* on KV, numbers and lengths of cilia from siblings and mutants were determined as described in the Materials and methods. We analyzed 882 cilia in 25 embryos (14 siblings and 11 mutants) but we did not observe a significant difference in cilia number (P>0.28) or length (P>0.19) between siblings and mutants (3.45±0.53 μm in length and 32±18 cilia per KV in siblings versus 3.20±0.33 μm in length and 40±17 cilia per KV in mutants, two-tailed student t-test applied).

Interestingly, although the cilia in the pronephros of *sea* mutants are predominantly immotile, cilia motility in KV of *sea* mutants is highly variable, based on the movement of beads injected to analyze flow. We chose to analyze embryos from two different *sea* backgrounds as the level of defects can vary from clutch to clutch. The pair *sea*^{tg238a}-C produces a higher level of left-right patterning defects (28%) (see Table S1 in the supplementary material) compared with the pair *sea*^{fa20r}-M21, which produces a lower level (2%) (see Table S1 in the supplementary material). We predicted that flow would be more severely affected in mutant embryos from pair C than from pair M21, and this is what we observe (Table 4). In *sea*^{tg238}mutants, one out of five embryos had strong counter-clockwise flow, whereas four out of five showed reduced or absent flow. In *sea*^{fa20r} mutants, five out of eight embryos had strong counter-clockwise flow, whereas three out of eight showed reduced or absent flow (see Movies 11-13 in the supplementary material). However, defects in flow did not always correlate with defects in heart looping. Some embryos with strong flow were found to have incorrect heart looping, whereas other embryos with defects in flow had correct heart looping. This suggests that Sea may affect left-right patterning both by affecting flow and through additional undetermined mechanisms that are independent of flow.

seahorse mutants are hypomorphic

One possible explanation for why *sea* mutants display lower than expected left-right patterning defects, is that maternal contribution of Lrrc6l can compensate for the zygotic mutations in this process. We find *sea* is provided maternally (Fig. 3A) and maternal Sea protein can be detected at low levels in 27 hpf fish (Kishimoto et al., 2008). As the role for cilia in left-right patterning probably occurs prior to this point at ~12-14 hpf, maternal contribution of Sea could influence this event. We have not been able to formally test this hypothesis as we have not been able to generate a functional translational start site morpholino to knock-down maternal message without causing additional phenotypes (B.X. and R.D.B., unpublished) (Kishimoto et al., 2008).

Another explanation for why *sea* mutants have weak effects on left-right patterning is that the point mutations do not completely eliminate *sea* function. To test this hypothesis, we examined whether the knockdown of *sea* mRNA using splice-site morpholino antisense oligonucleotides (MOs) produces the same left-right patterning phenotypes observed in mutants. Splice-site morpholinos typically affect only zygotic message and thus should produce comparable phenotypes with zygotic mutants. Sea MO-injected embryos have a higher level of defects in visceral organ placement compared with *sea* mutants ($P<3\times10^{-5}$ or

Table 2. Left-right patterning phenotypes in *sea* mutants and morphants

			Visceral organ asymmetry (%)			
Genotype	Stage	*n*	SS	SI	Heterotaxic	Abnormal
sea^{tg238a} siblings (+/+, +/–)	48 hpf	426	98	1	1	–
sea^{tg238a} –/–	48 hpf	429	89	4	7	–
sea^{fa20r} siblings (+/+, +/–)	48 hpf	400	99	1	–	–
sea^{fa20r} –/–	48 hpf	249	91	6	3	–
Wild-type uninjected	48 hpf	52	96	4	–	–
Wild type + e5i5 sea MO	48 hpf	148	56	22	14	8
			Asymmetric gene expression (%)			
			L	R	B	None
sea^{tg238a} clutch	20 s	248	93	1	6	–
sea^{tg238a} –/–	20 s	62	82	3	15	–
sea^{fa20r} clutch	20 s	219	93	1	6	–
sea^{fa20r} –/–	20 s	55	87	2	11	–
Wild-type uninjected	20 s	74	97	3	–	–
Wild type + e5i5 sea MO	20 s	66	50	33	17	–

hpf, hours post fertilization; SS, situs solitus (wild type), SI situs inversus (reversed); s, somites; L, left; R, right; B, bilateral.
We determined visceral organ asymmetry based on the position of the heart, liver and pancreas as described previously (Schottenfeld et al., 2007) (see Fig. S1 in the supplementary material). Heterotaxic refers to a random arrangement of organs; thus, not SS or SI. Abnormal refers to malformation of organs that was observed occasionally in MO injected embryos. Asymmetric gene expression refers to combined numbers for *southpaw, lefty1* and *lefty2* expression.
At 48 hpf, –/– embryos were selected on the basis of the curly tail down phenotype. At 20 s, it is not possible to distinguish mutants from siblings morphologically. All embryos with abnormal asymmetric gene expression at 20 s were genotyped. The number of –/– embryos with left expression was extrapolated from the total value on the basis that mutants make up ~25% of the clutch.

$P<5\times10^{-6}$ for *sea*^{tg238} and *sea*^{fa20r}, respectively, Chi-Square analysis applied). A higher percentage of sea MO-injected embryos also have defects in asymmetric gene expression compared with *sea* mutants (Table 2). These results suggest that the *sea* mutant alleles are hypomorphic and that mutant proteins retain some function that is eliminated by MO knockdown.

To further test this hypothesis, we injected a suboptimal dose of MO, which does not cause significant curly tail defects on its own, and assayed for enhancement of left-right phenotypes in *sea* mutants. We injected clutches from *sea* heterozygous parents and separated embryos on the basis of CTD phenotypes at 27 hpf and then on the basis of heart looping defects at 50 hpf, followed by genotyping. Although uninjected controls had the expected 25% CTD phenotypes and a low level of heart looping defects, the MO-injected clutches had higher percentages in both categories (Table 5; total numbers for injected and uninjected clutches). When separated by genotype, it is clear that the MO enhances the left-right patterning phenotypes in mutant embryos. In addition, the injection of the MO into heterozygous embryos produces a tail curl that is indistinguishable from mutants.

Sea mutants retain their ability to interact with Disheveled

An insertional allele of Sea was described recently that causes left-right patterning and kidney defects. But, in contrast to our alleles, this insertional allele does not affect cilia motility (Kishimoto et al., 2008). Kishimoto et al. found that Sea participates in Wnt/PCP signaling and interacts with Disheveled (Dsh). Loss of Dsh in *Xenopus* leads to mispositioned basal bodies and defects in ciliogenesis (Park et al., 2008). In theory, Sea could participate with Dsh to control these aspects of cilia function.

To determine whether our mutant alleles affect the ability of Sea to interact with Dsh, we performed co-immunoprecipitation experiments with epitope-tagged Sea and Dsh constructs. Both Sea mutant proteins retained the ability to interact with Dsh in this assay, although Sea^{fa20r} shows a reduced ability to bind Dsh (Fig. 6). This could indicate that the truncation in this protein affects the Dsh-binding domain. Our mutants do not affect ciliogenesis, as is seen in Dsh loss of function (Park et al., 2008), suggesting that the interaction between mutant Sea and Dsh does not eliminate Dsh function in ciliogenesis. Furthermore, TEM analysis of Sea mutants demonstrates that cilia have correct apically positioned basal bodies (Fig. 4Q), which are incorrectly positioned in *Xenopus* embryos lacking Dsh function (Park et al., 2008). Thus, the ability of our *sea* alleles to affect cilia motility appears to be independent of interaction with Dsh.

DISCUSSION

seahorse (*lrrc6l*) is involved in cilia motility and pronephric cyst formation Defect

We describe the phenotypes associated with two point mutations in *seahorse*, a gene encoding the leucine-rich repeat-containing protein Lrrc6l. We show that *sea* is required for correct cilia motility in the pronephros and that mutants show subsequent dilations in the tubules, consistent with other mutants that affect cilia motility, including one involving another leucine-rich repeat-containing

Table 3. Left-right patterning phenotypes in the diencephalon of *sea* mutants

			Habenula asymmetry (*lov* expression %)		
Genotype	Stage	*n*	Left (normal)	Right (reversed)	Bilateral (isomeric)
sea^{tg238a} (+/+, +/–)	4 dpf	1067	96	2	2
sea^{tg238} (–/–)	4 dpf	414	71	24	5
sea^{fa20r} (+/+, +/–)	4 dpf	275	97	2	1
sea^{fa20r} (–/–)	4 dpf	94	83	15	2

Table 4. Fluid flow in Kupffer's vesicle of *sea* mutants

Genotype	*n*	Strong flow	Reduced flow	Absent flow
sea^{tg238a} (+/+, +/–)	4	3 (1)	1 (1)	–
sea^{tg238} (–/–)	5	1 (1)	1 (0)	3 (1)
sea^{fa20r} (+/+, +/–)	8	8 (6)	–	–
sea^{fa20r} (–/–)	8	5 (4)	1 (1)	2 (1)

The *tg238a*/+ pair used to produce the embryos for this experiment (*tg238a-C*) have a high degree of left-right patterning defects (28%). The *fa20r*/+ pair used to produce the embryos for this experiment (*fa20r-M21*) have a low degree of left-right patterning defects (2%). See Table S1 for details. Numbers in parentheses indicate embryos with correct heart looping in each category.

protein Lrrc50 (Kramer-Zucker et al., 2005; Omori and Malicki, 2006; Sullivan-Brown et al., 2007; Zhao and Malicki, 2007; van Rooijen et al., 2008). We first see dilations in the area we refer to as the medial tubules (this report) (Sullivan-Brown et al., 2007). This area of the zebrafish pronephros is analogous to the proximal convoluted and straight tubules (Wingert et al., 2007), a region where cysts occur in human disease (Nakanishi et al., 2000).

It is important to note that the pronephric cyst phenotypes we observe in our *sea* alleles strongly resemble those reported for an insertional allele of *sea* (Kishimoto et al., 2008). Intriguingly, the insertional allele does not affect cilia motility, whereas both of our alleles have a strong affect on motility. Although work has convincingly shown that defects in fluid flow can results in pronephric dilations in zebrafish (Kramer-Zucker et al., 2005), the phenotype of the *sea* insertional mutant strongly suggests that kidney cyst formation in zebrafish can be separable from cilia motility defects. Thus, our alleles of Sea may affect both cilia motility and pronephric cyst formation through different mechanisms.

Defects in cilia motility and/or flow do not correlate with left-right axis defects

As cilia motility in KV is important for proper left-right patterning (Essner et al., 2005; Kramer-Zucker et al., 2005), zebrafish mutations affecting cilia motility are predicted to have strong effects on left-right patterning. Intriguingly, we observe that *sea* mutants have a weak effect on left-right patterning. One possibility for this finding is that left-right patterning is an early developmental event and may be influenced by the maternal contribution of Lrrc6l. We believe this is likely, but we have been unable to generate the appropriate tools to test this. A second possibility is that some residual function of Sea remains in the mutant embryos. In support of *sea* alleles being hypomorphic, we can obtain a stronger effect of *sea* on left-right patterning using MO antisense knockdown. Interestingly, in our experiment the addition of a suboptimal dose of MO to *sea* heterozygotes produced curly tail down phenotypes that were indistinguishable from *sea* mutants. Taken together, these results suggest that embryos are sensitive to the amount of Lrrc6l that is present and that the hypomorphic alleles may result in variable phenotypes depending on the amount of maternal protein present coupled with influences from the genetic background. We have noticed that the penetrance of left-right patterning defects in *sea* can vary depending on the background and age of the parents (see Table S1 in the supplementary material). However in our alleles, we have not observed variability in pronephric cyst formation or cilia motility defects in the pronephros and neural tube.

A more intriguing possibility to explain why mutations that affect cilia motility do not cause pronounced left-right patterning defects is that these functions may be separable, similar to what we describe above for pronephric phenotypes. We do find that our *sea* alleles affect KV cilia motility and flow, but embryos with obvious defects in flow do not consistently show defects in heart looping. We also find that embryos with defects in heart looping often have flow that resembles wild type. An explanation for these results is that these defects in flow are not severe enough to consistently influence asymmetric patterning. This explanation is intriguing, as mutations in mouse that cause subtle defects in cilia motility, such as *inv*, still have profound effects on left-right patterning (Okada et al., 1999). Further studies on *sea* mutants could help determine what elements of flow are absolutely crucial to left-right patterning. Alternatively, *inv* mutations have also been implicated in Wnt signaling and it may be this function that is more crucial to left-right patterning (Simons et al., 2005). As Sea interacts with Dsh and is involved in Wnt/PCP signaling (Kishimoto et al., 2008), it is intriguing to speculate that the function of Sea in this pathway is more crucial to left-right patterning and pronephric cyst formation. The PCP pathway may act in parallel to flow, suggesting that whereas flow is somewhat affected in *sea* mutants, the more crucial role for *sea* may lie in a different aspect of left-right axis determination.

Table 5. Heart looping and tail curl phenotypes of *sea* embryos injected with a low dose of sea MO

			Heart looping (%)			Tail phenotypes (%)		
Genotype	Stage	*n*	Right (normal)	Left (reversed)	None (midline)	Straight	Slight bend	CTD
sea^{tg238a} (+/+, +/–)	50 hpf	451	99	1	0	100	–	–
sea^{tg238a} (–/–)	50 hpf	150	92	7	1	–	–	100
sea^{tg238a} + e5i5 sea MO (+/+)	50 hpf	29	76	24	–	100	–	–
sea^{tg238a} + e5i5 sea MO (+/–)	50 hpf	101	73	27	–	59	21	20
sea^{tg238a} + e5i5 sea MO (–/–)	50 hpf	23	52	48	–	–	17	83
sea^{fa20r} (+/+, +/–)	50 hpf	370	100	–	–	100	–	–
sea^{fa20r} (–/–)	50 hpf	120	94	5	2	–	–	100
sea^{fa20r} + e5i5 sea MO (+/+)	50 hpf	10	90	10	–	20	80	–
sea^{fa20r} + e5i5 sea MO (+/–)	50 hpf	25	68	32	–	36	44	20
sea^{fa20r} + e5i5 sea MO (–/–)	50 hpf	12	75	25	–	–	–	100

CTD, curly tail down.
Clutches of *sea* embryos were injected with a low dose of sea MO that does not cause CTD defects on its own. Injected embryos were scored for tail curl and heart looping followed by genotyping. 'slight bend' refers to embryos where the tails were not perfectly straight but had small bends or kinks at the end. This phenotype is easily distinguishable from the true CTD phenotype.

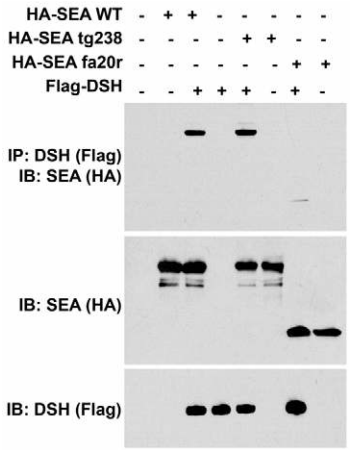

Fig. 6. *seahorse* mutants retain the ability to interact with Dsh. Upper panel: western blot with anti-HA on samples pulled down by immunoprecipiatation with anti-Flag. Middle and lower panels are western blots of lysates with the indicated antibody to visualize the input of Sea proteins (HA) or Dsh (Flag). Note that both *sea*^{tg238a} and *sea*^{fa20r} can produce stable proteins in vivo. Both mutant Sea proteins can interact with Dsh, although the weaker interaction seen with Sea^{fa20r} may indicate that the truncation in this protein affects the binding site for Dsh.

Leucine-rich repeat proteins and cilia motility

Lrrc6l is conserved in mammals, flies and the single-celled algae, *Chlamydomonas*, but not in *C. elegans* (Avidor-Reiss et al., 2004). As *C. elegans* do not have motile cilia, *lrrc6l* was placed in a subset of genes required for cilia motility. Orthologs to *sea* also exist in the flagellated protozoan *Trypanomsoma brucei*, where RNA interference results in aberrant basal body replication and flagellar biogenesis, resulting in a subsequent reduction of cell size (Morgan et al., 2005). In humans and mice, Lrrc6l was identified as a testis-specific protein, most abundantly expressed in pachytene and diplotene cells in meiosis I (Xue and Goldberg, 2000). Furthermore, mutations in *sea* have been identified in different screens in zebrafish to cause cystic kidneys and defects in the kinocilia on hair cells (McDermott et al., 2007; Sun et al., 2004). Thus, the function of Lrcc6l appears to be conserved in processes involving cilia/flagella.

The cilia proteome currently contains 14 proteins with leucine-rich repeats (including Lrrc6l) out of over 1200 proteins identified as being found in cilia or basal bodies (Gherman et al., 2006). The architecture of Lrrc6l places it in the SDS22-like subfamily. Proteins in this family are diverse in function, but include splicing factors and nuclear export proteins (Kobe and Kajava, 2001). Interestingly, Lrrc6l has putative nuclear import/export sequences, suggesting that this protein may have functions inside the nucleus.

Recently, another LRR containing protein in zebrafish, which we call *switch hitter* (*lrrc50*), has been shown to affect cilia motility, cause kidney cysts and strongly affect left-right patterning (Sullivan-Brown et al., 2007; van Rooijen et al., 2008) (J.S.-B., K.B. and R.D.B., unpublished). The number and position of the LRRs and coiled coil domain in Lrrc6l are similar in position to those in Lrrc50. LRR and coiled-coil domains often act as protein-protein interactions domains, suggesting that Lrrc6l and Lrrc50 may act as scaffolding proteins. Work on the Lrrc50 ortholog Oda7 in *Chlamydomonas* suggests this protein acts to interconnect outer and inner row dyneins and coordinate their functions (Freshour et al., 2007). However there is additional evidence that Oda7 may also act in the cytoplasm to allow for the proper assembly of outer row dynein complexes bound for the cilium (Freshour et al., 2007). Recent work finds that Lrrc6l is expressed in the cytoplasm and not the cilium or centriole (Kishimoto et al., 2008). Lrrc6l and Lrrc50 have similar domains arrangements; thus, we hypothesize that Lrrc6l may be functioning analogously to Lrrc50 in the cytoplasm to allow for correct assembly of protein complexes bound for the cilium. *oda7*/*lrrc50* mutations result in the loss of outer dynein arms in the cilium, which explains why mutations in this gene affect cilia motility (Freshour et al., 2007; van Rooijen et al., 2008). As we do not see defects in cilia structure in *sea* mutants, it will be interesting to determine what Lrrc6l interacts with in order to affect cilia motility. Our current work suggests that interactions with Dsh are not affected in our alleles, suggesting other interacting partners may be important for cilia motility. Given that mutations in both *lrrc6l* and *lrrc50* affect cilia motility, it will be interesting to determine whether the other 12 leucine-rich repeat proteins in the cilia proteome play similar roles in cilia function, kidney cystogenesis and left-right patterning. Additionally, it will be important to determine whether any of these proteins are acting redundantly, perhaps compensating for loss of Sea in KV but not in the pronephros.

We thank Robert Geisler and Silke Geiger-Rudolph for the original bulked segregant analysis that placed *sea*^{tg238a} on chromosome 2; John Mably for advice on positional cloning; Christine Hostetter, Heather McAllister and Jaclyn Taylor for zebrafish care; Peggy Bisher for assistance with TEM; Stephan Y. Thiberge for assistance with video microscopy; Ray Habas for *disheveled* constructs; and the members of the Burdine and Fishman laboratories for helpful discussions. We thank Jonathan Eggenschwiler, Jack Lee, Kim Poole and Jodi Schottenfeld for participating in the blind test of KV flow. J.S.B. is supported by predoctoral award 05-2411-CCR-E0 from the New Jersey Commission on Cancer Research. S.-Y.L. is supported by a Graduate Research Fellowship from the National Science Foundation. K.M.J. is supported by postdoctoral grant 0825952D from the American Heart Association. R.D.B. is the 44th Scholar of the Edward Mallinckrodt Jr Foundation, and funds from this award were used in support of this work. Funds from awards to R.D.B. from the New Jersey Commission on Cancer Research (04-2405-CCR-E0), from the Polycystic Kidney Disease Foundation, (#117b2r) and from the National Institutes of Child Health and Human Development (1R01HD048584) were used in support of this work. Video imaging was performed in the Princeton Imaging Facility, which is supported by grant P50GM071508 from NIH/NIGMS. Deposited in PMC for release after 12 months.

Supplementary material

Supplementary material available online at
http://dev.biologists.org/cgi/content/full/136/10/1621/DC1

References

Avidor-Reiss, T., Maer, A. M., Koundakjian, E., Polyanovsky, A., Keil, T., Subramaniam, S. and Zuker, C. S. (2004). Decoding cilia function: defining specialized genes required for compartmentalized cilia biogenesis. *Cell* **117**, 527-539.

Bisgrove, B. W. and Yost, H. J. (2006). The roles of cilia in developmental disorders and disease. *Development* **133**, 4131-4143.

Bisgrove, B. W., Essner, J. J. and Yost, H. J. (1999). Regulation of midline development by antagonism of lefty and nodal signaling. *Development* **126**, 3253-3262.

Bollig, F., Mehringer, R., Perner, B., Hartung, C., Schafer, M., Schartl, M., Volff, J. N., Winkler, C. and Englert, C. (2006). Identification and comparative expression analysis of a second wt1 gene in zebrafish. *Dev. Dyn.* **235**, 554-561.

Brand, M., Heisenberg, C. P., Warga, R. M., Pelegri, F., Karlstrom, R. O., Beuchle, D., Picker, A., Jiang, Y. J., Furutani-Seiki, M., van Eeden, F. J. et al. (1996). Mutations affecting development of the midline and general body shape during zebrafish embryogenesis. *Development* **123**, 129-142.

Ceulemans, H., De Maeyer, M., Stalmans, W. and Bollen, M. (1999). A capping domain for LRR protein interaction modules. *FEBS Lett.* **456**, 349-351.

Chen, J.-N., van Bebber, F., Goldstein, A. M., Serluca, F. C., Jackson, D., Childs, S., Serbedzija, G., Warren, K. S., Mably, J. D., Lindahl, P. et al.

(2001). Genetics steps to organ laterality in zebrafish. *Comp. Funct. Genom.* **2**, 60-68.
Drummond, I. (2003). Making a zebrafish kidney: a tale of two tubes. *Trends Cell Biol.* **13**, 357-365.
Essner, J. J., Amack, J. D., Nyholm, M. K., Harris, E. B. and Yost, H. J. (2005). Kupffer's vesicle is a ciliated organ of asymmetry in the zebrafish embryo that initiates left-right development of the brain, heart and gut. *Development* **132**, 1247-1260.
Fliegauf, M., Benzing, T. and Omran, H. (2007). When cilia go bad: cilia defects and ciliopathies. *Nat. Rev. Mol. Cell. Biol.* **8**, 880-893.
Freshour, J., Yokoyama, R. and Mitchell, D. R. (2007). Chlamydomonas flagellar outer row dynein assembly protein ODA7 interacts with both outer row and I1 inner row dyneins. *J. Biol. Chem.* **282**, 5404-5412.
Gamse, J. T., Thisse, C., Thisse, B. and Halpern, M. E. (2003). The parapineal mediates left-right asymmetry in the zebrafish diencephalon. *Development* **130**, 1059-1068.
Gherman, A., Davis, E. E. and Katsanis, N. (2006). The ciliary proteome database: an integrated community resource for the genetic and functional dissection of cilia. *Nat. Genet.* **38**, 961-962.
Habas, R., Kato, Y. and He, X. (2001). Wnt/Frizzled activation of Rho regulates vertebrate gastrulation and requires a novel Formin homology protein Daam1. *Cell* **107**, 843-854.
Kishimoto, N., Cao, Y., Park, A. and Sun, Z. (2008). Cystic kidney gene seahorse regulates cilia-mediated processes and Wnt pathways. *Dev. Cell* **14**, 954-961.
Kobe, B. and Kajava, A. V. (2001). The leucine-rich repeat as a protein recognition motif. *Curr. Opin. Struct. Biol.* **11**, 725-732.
Kramer-Zucker, A. G., Olale, F., Haycraft, C. J., Yoder, B. K., Schier, A. F. and Drummond, I. A. (2005). Cilia-driven fluid flow in the zebrafish pronephros, brain and Kupffer's vesicle is required for normal organogenesis. *Development* **132**, 1907-1921.
Krauss, S., Johansen, T., Korzh, V. and Fjose, A. (1991). Expression of the zebrafish paired box gene pax[zf-b] during early neurogenesis. *Development* **113**, 1193-1206.
Liao, E. C. and Zon, L. I. (1999). Simple sequence-length polymorphism analysis. *Methods Cell Biol.* **60**, 181-183.
Liu, Y., Pathak, N., Kramer-Zucker, A. and Drummond, I. A. (2007). Notch signaling controls the differentiation of transporting epithelia and multiciliated cells in the zebrafish pronephros. *Development* **134**, 1111-1122.
Long, S., Ahmad, N. and Rebagliati, M. (2003). The zebrafish nodal-related gene southpaw is required for visceral and diencephalic left-right asymmetry. *Development* **130**, 2303-2316.
Ma, M. and Jiang, Y. J. (2007). Jagged2a-notch signaling mediates cell fate choice in the zebrafish pronephric duct. *PLoS Genet.* **3**, e18.
Majumdar, A. and Drummond, I. A. (2000). The zebrafish floating head mutant demonstrates podocytes play an important role in directing glomerular differentiation. *Dev. Biol.* **222**, 147-157.
McDermott, B. M., Jr, Baucom, J. M. and Hudspeth, A. J. (2007). Analysis and functional evaluation of the hair-cell transcriptome. *Proc. Natl. Acad. Sci. USA* **104**, 11820-11825.
Milewski, W. M., Duguay, S. J., Chan, S. J. and Steiner, D. F. (1998). Conservation of PDX-1 structure, function, and expression in zebrafish. *Endocrinology* **139**, 1440-1449.
Morgan, G. W., Denny, P. W., Vaughan, S., Goulding, D., Jeffries, T. R., Smith, D. F., Gull, K. and Field, M. C. (2005). An evolutionarily conserved coiled-coil protein implicated in polycystic kidney disease is involved in basal body duplication and flagellar biogenesis in Trypanosoma brucei. *Mol. Cell. Biol.* **25**, 3774-3783.
Nakanishi, K., Sweeney, W. E., Jr, Zerres, K., Guay-Woodford, L. M. and Avner, E. D. (2000). Proximal tubular cysts in fetal human autosomal recessive polycystic kidney disease. *J. Am. Soc. Nephrol.* **11**, 760-763.
Odenthal, J. and Nusslein-Volhard, C. (1998). fork head domain genes in zebrafish. *Dev. Genes Evol.* **208**, 245-258.
Ohara, O., Dorit, R. L. and Gilbert, W. (1989). One-sided polymerase chain reaction: the amplification of cDNA. *Proc. Natl. Acad. Sci. USA* **86**, 5673-5677.
Ohkura, H. and Yanagida, M. (1991). S. pombe gene sds22+ essential for a midmitotic transition encodes a leucine-rich repeat protein that positively modulates protein phosphatase-1. *Cell* **64**, 149-157.
Okabe, N., Xu, B. and Burdine, R. D. (2008). Fluid dynamics in zebrafish Kuppfer's vesicle. *Dev. Dyn.* **237**, 3602-3612.
Okada, Y., Nonaka, S., Tanaka, Y., Saijoh, Y., Hamada, H. and Hirokawa, N. (1999). Abnormal nodal flow precedes situs inversus in iv and inv mice. *Mol. Cell* **4**, 459-468.
Omori, Y. and Malicki, J. (2006). oko meduzy and related crumbs genes are determinants of apical cell features in the vertebrate embryo. *Curr. Biol.* **16**, 945-957.
Park, T. J., Mitchell, B. J., Abitua, P. B., Kintner, C. and Wallingford, J. B. (2008). Dishevelled controls apical docking and planar polarization of basal bodies in ciliated epithelial cells. *Nat. Genet.* **40**, 871-879.
Praetorius, H. A. and Spring, K. R. (2005). A physiological view of the primary cilium. *Annu. Rev. Physiol.* **67**, 515-529.
Schottenfeld, J., Sullivan-Brown, J. and Burdine, R. D. (2007). Zebrafish curly up encodes a Pkd2 ortholog that restricts left-side-specific expression of southpaw. *Development* **134**, 1605-1615.
Serluca, F. C. and Fishman, M. C. (2001). Pre-pattern in the pronephric kidney field of zebrafish. *Development* **128**, 2233-2241.
Simons, M., Gloy, J., Ganner, A., Bullerkotte, A., Bashkurov, M., Kronig, C., Schermer, B., Benzing, T., Cabello, O. A., Jenny, A. et al. (2005). Inversin, the gene product mutated in nephronophthisis type II, functions as a molecular switch between Wnt signaling pathways. *Nat. Genet.* **37**, 537-543.
Sullivan-Brown, J., Schottenfeld, J., Okabe, N., Hostetter, C. L., Serluca, F. C., Thiberge, S. Y. and Burdine, R. D. (2007). Zebrafish mutations affecting cilia motility share similar cystic phenotypes and suggest a mechanism of cyst formation that differs from pkd2 morphants. *Dev. Biol.* **314**, 261-275.
Sun, Z., Amsterdam, A., Pazour, G. J., Cole, D. G., Miller, M. S. and Hopkins, N. (2004). A genetic screen in zebrafish identifies cilia genes as a principal cause of cystic kidney. *Development* **131**, 4085-4093.
Thisse, C., Thisse, B., Schilling, T. F. and Postlethwait, J. H. (1993). Structure of the zebrafish snail1 gene and its expression in wild-type, spadetail and no tail mutant embryos. *Development* **119**, 1203-1215.
van Rooijen, E., Giles, R. H., Voest, E. E., van Rooijen, C., Schulte-Merker, S. and van Eeden, F. J. (2008). LRRC50, a conserved ciliary protein implicated in polycystic kidney disease. *J. Am. Soc. Nephrol.* **19**, 1128-1138.
Wingert, R. A., Selleck, R., Yu, J., Song, H. D., Chen, Z., Song, A., Zhou, Y., Thisse, B., Thisse, C., McMahon, A. P. et al. (2007). The cdx genes and retinoic acid control the positioning and segmentation of the zebrafish pronephros. *PLoS Genet.* **3**, 1922-1938.
Xue, J. C. and Goldberg, E. (2000). Identification of a novel testis-specific leucine-rich protein in humans and mice. *Biol. Reprod.* **62**, 1278-1284.
Yelon, D., Horne, S. A. and Stainier, D. Y. (1999). Restricted expression of cardiac myosin genes reveals regulated aspects of heart tube assembly in zebrafish. *Dev. Biol.* **214**, 23-37.
Yoder, B. K. (2007). Role of primary cilia in the pathogenesis of polycystic kidney disease. *J. Am. Soc. Nephrol.* **18**, 1381-1388.
Zhao, C. and Malicki, J. (2007). Genetic defects of pronephric cilia in zebrafish. *Mech. Dev.* **124**, 605-616.